J Solid State Electrochem (2000) 4: 394–401

ORIGINAL PAPER

Milivoj Lovrić · Michael Hermes · Fritz Scholz

Solid state electrochemical reactions in systems with miscibility gaps

Received: 14 October 1999 / Accepted: 4 November 1999

Abstract Cyclic voltammograms of electroactive solid compounds with partial immiscibility between the oxidized and reduced phases can exhibit a splitting of the peaks. If the free energy of transformation between the oxidized and reduced phases is small, the formal potentials of the redox pair will be almost the same in both solid phases. This results in an inert potential range in which no appreciable electrochemical activity is possible. The kinetic implications of this situation have been analysed in relation to the width of the miscibility gap. The diffusion of ions in the particle, which is hindered by the immiscibility, can proceed when a transition zone between the two phases exists in which the crystal structure is changed. If there is no such transition zone the voltammogram will display several spikes, which are caused by the collapse of concentration barriers at the sharp interfaces between the two phases in the mixed crystals.

Key words Miscibility gap · Mixed phases · Cyclic voltammetry · Solid state electrochemistry

Introduction

In a previous paper, the role of redox mixed phases in solid state electrochemical reactions and the effects of miscibility gaps in the voltammetry of microcrystals were discussed [1]. In this communication, the dependence of the voltammetric response on the difference in the formal potentials of separate phases and the influence of the limited miscibility of redox components on the mass transfer in solid particles are analysed theoretically.

A reversible redox reaction between the oxidized and the reduced forms of a certain solid compound, accompanied by the insertion of a cation C^+ from the solution into the particle, is considered:

$$\{\mathrm{ox}\} + n\mathrm{e}^- + n\mathrm{C}^+ \rightleftharpoons \{\mathrm{C}_n\mathrm{red}\} \quad (1)$$

where species in braces are confined to the solid phase. In equilibrium, the composition of the solid phase is determined by the electrode potential, according to the Nernst equation [2]:

$$E = E_\mathrm{f}^\circ + (RT/nF)\ln(a_{\{\mathrm{ox}\}}/a_{\{\mathrm{C}_n\mathrm{red}\}}) \quad (2)$$

where

$$E_\mathrm{f}^\circ = E_{\mathrm{ox/red}}^\circ + (RT/nF)\ln(K) + (RT/F)\ln([\mathrm{C}^+]^*)$$

is the formal potential of the redox reaction [3], $[C^+]^*$ is the activity of cations in the bulk of the solution, $E_{\mathrm{ox/red}}^\circ$ is the standard potential of the partial redox reaction

$$\{\mathrm{ox}\} + n\mathrm{e}^- \rightleftharpoons \{\mathrm{red}^{n-}\} \quad (3)$$

and K is an equilibrium constant of the ion-transfer reaction

$$\{\mathrm{red}^{n-}\} + n\mathrm{C}^+ \rightleftharpoons \{\mathrm{C}_n\mathrm{red}\} \quad (4)$$

It is assumed that the activities of redox components of the solid compound are proportional to their molar fractions in the mixed crystal [4]. A miscibility gap may appear if these two components cannot be mixed in all ratios. If $\{ox\}$ is gradually reduced to $\{C_nred\}$, the activity of $\{C_nred\}$ may increase up to a certain limiting value:

$$Z_{\mathrm{Cred/ox}} = (m_{\mathrm{C}_n\mathrm{red}})_\mathrm{lim}/[(m_{\mathrm{C}_n\mathrm{red}})_\mathrm{lim} + m_\mathrm{ox}] \quad (5)$$

which depends on the maximum solubility of $\{C_nred\}$ in $\{ox\}$. Then the activity of $\{ox\}$ can be abruptly changed to the other limiting value:

M. Lovrić (✉)
Center for Marine Research "Rudjer Boškovic" Institute,
POB 180, 10002 Zagreb, Croatia

M. Hermes · F. Scholz
Institut für Chemie und Biochemie,
Ernst-Moritz-Arndt Universität, Soldtmannstrasse 23,
17489 Greifswald, Germany

$$Z_{\mathrm{ox/Cred}} = (m_{\mathrm{ox}})_{\mathrm{lim}}/[(m_{\mathrm{ox}})_{\mathrm{lim}} + m_{\mathrm{C}_n\mathrm{red}}] \quad (6)$$

which depends on the maximum solubility of {ox} in {$C_n$red}. Here m_{ox} and $m_{\mathrm{C}_n\mathrm{red}}$ are numbers of moles of {ox} and {$C_n$red}, respectively. This abrupt change of the composition requires a massive ingress of ions into the solid phase [5]. In this paper, a model of this process is developed for cyclic voltammetry using a lattice-gas concept without interactions.

Theory

It is assumed that a small cylinder of the redox active substance is pressed into an electrode surface in such a way that only one of its surfaces is exposed to the solution (see Fig. 1). The substance is a good electronic conductor and its surface, which is in contact with the solution, acquires the electrode potential at the very beginning of the experiment. Cations can diffuse through this surface along the longitudinal axis x of the cylinder. So, the mass transfer can be described by the planar diffusion model:

$$\partial c/\partial t = D(\partial^2 c/\partial x^2) \quad (7)$$

where c is the molar concentration of the oxidized component {ox}. The starting and the boundary conditions for the perfect miscibility are the following:

$$\begin{aligned} t = 0,\ x \geq 0: &\quad c = \rho \\ t > 0,\ x = 0: &\quad c/\rho = \exp(\phi)[1 + \exp(\phi)]^{-1} \\ &\quad \partial c/\partial x = I/nFSD \\ x = l: &\quad \partial c/\partial x = 0 \end{aligned} \quad (8)$$

where ρ is a density of the solid compound in mol/cm^3, $\phi = nF(E - E^{\circ}_{\mathrm{f}})/RT$ is a dimensionless electrode potential, S is the area of the solid particle surface which is exposed to the solution, D is a diffusion coefficient of ions C^+ in the crystal lattice, l is a thickness of the cylinder and I is a current. Equation (7) was solved by the finite difference method [6]:

$$f = 2d(c(1) - c(0)) \quad (9)$$

$$\Delta c(1) = d(c(2) - c(1)) - f \quad (10)$$

$$\Delta c(j) = d(c(j+1) + c(j-1) - 2c(j)) \quad (11)$$

$$\Delta c(n) = d(c(n-1) - c(n)) \quad (12)$$

where $2 \leq j < n$, $d = D\Delta t/\Delta x^2$ and $f = I\Delta t/nFS\rho\Delta x$.

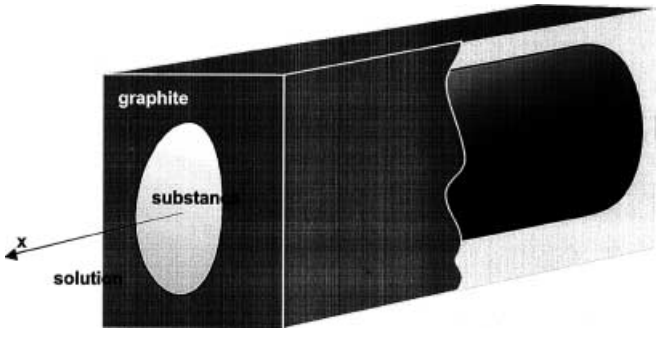

Fig. 1 Substance cylinder embedded in graphite, and in contact with the electrolyte phase. The three-phase junction is the line surrounding the exposed cylinder surface (planar diffusion model)

The limited miscibility was simulated by putting $c(0) = \exp(\phi)[1 + \exp(\phi)]^{-1}$ if $c(0) \geq 1 - Z_{\mathrm{Cred/ox}}$, or $c(0) \leq Z_{\mathrm{ox/Cred}}$. If $Z_{\mathrm{ox/Cred}} < \exp(\phi)[1 + \exp(\phi)]^{-1} < 1 - Z_{\mathrm{Cred/ox}}$, then $c(0) = 1 - Z_{\mathrm{Cred/ox}}$ in the cathodic branch, and $c(0) = Z_{\mathrm{ox/Cred}}$ in the anodic branch of the cyclic voltammogram. If similar conditions are imposed upon all concentrations, they may create concentration barriers in the particle:

$$c(j) < Z_{\mathrm{ox/Cred}} \quad (13)$$

$$c(j+1) = 1 - Z_{\mathrm{Cred/ox}} \quad (14)$$

where $0 < Z_{\mathrm{ox/Cred}} < 0.5$ and $0 < Z_{\mathrm{Cred/ox}} < 0.5$. The magnitude of the barrier is:

$$b = 1 - Z_{\mathrm{Cred/ox}} - Z_{\mathrm{ox/Cred}} \quad (15)$$

In the cathodic branch of the cyclic voltammogram the barrier can collapse if:

$$c(j) + \Delta c(j) < Z_{\mathrm{ox/Cred}} \quad (16)$$

$$c(j+1) + \Delta c(j+1) = Z_{\mathrm{ox/Cred}} \quad (17)$$

where $\Delta c(j) = d(c(j+1) - c(j))$ and $\Delta c(j+1) = -\Delta c(j)$. Equations (16) and (17) are simplified by neglecting all other fluxes. In the anodic branch the barrier is the opposite:

$$c(j) > 1 - Z_{\mathrm{Cred/ox}} \quad (18)$$

$$c(j+1) = Z_{\mathrm{ox/Cred}} \quad (19)$$

It can collapse if:

$$c(j) + \Delta c(j) > 1 - Z_{\mathrm{Cred/ox}} \quad (20)$$

$$c(j+1) + \Delta c(j+1) = 1 - Z_{\mathrm{Cred/ox}} \quad (21)$$

The cyclic voltammetry was simulated using $d = 0.4$, $\Delta E = 0.0002$ V and $n = 100$. The number of space increments corresponded to nearly semi-infinite diffusion conditions: $c(n) > 0.95$ until the end of the cycle. The dimensionless current $\Phi = I(nFS\rho)^{-1}(DnFv/RT)^{-1/2}$, where $v = \Delta E/\Delta t$ is a scan rate, was calculated as a function of the electrode potential.

Results and discussion

In a previous communication, we introduced the concept of miscibility gaps to describe certain solid systems in which one reduced phase {$C_n$red} is transformed into an oxidized phase {ox} and vice versa [1]. We assumed that the initial oxidation of {$C_n$red} forms mixed crystals of composition {$\mathrm{ox}_x(C_n\mathrm{red})_{1-x}$} until the maximum solubility of {ox} in the reduced phase has been reached. The mixed crystal with this maximum concentration of {ox} may be formulated as {$\mathrm{ox}_{x'}(C_n\mathrm{red})_{1-x'}$}. Then there might exist a solubility gap until a composition of {$\mathrm{ox}_{y'}(C_n\mathrm{red})_{1-y'}$} has been reached (x′ is much smaller than y′) (see Fig. 2). The mixed crystal {$\mathrm{ox}_{y'}(C_n\mathrm{red})_{1-y'}$} is then further oxidized until {ox} is reached. The mixed phases {$\mathrm{ox}_x(C_n\mathrm{red})_{1-x}$} will have the structure α and the mixed phases {$\mathrm{ox}_y(C_n\mathrm{red})_{1-y}$} will have the structure β. α and β are so different in structure that a miscibility gap arises. The difference in Gibbs free energy $\Delta G_{\mathrm{A/B}}$ of the two phases {$\mathrm{ox}_{x'}(C_n\mathrm{red})_{1-x'}$} and {$\mathrm{ox}_{y'}(C_n\mathrm{red})_{1-y'}$} is equal to the difference in formal potentials of the redox system in the two phases and it can be split into two terms:

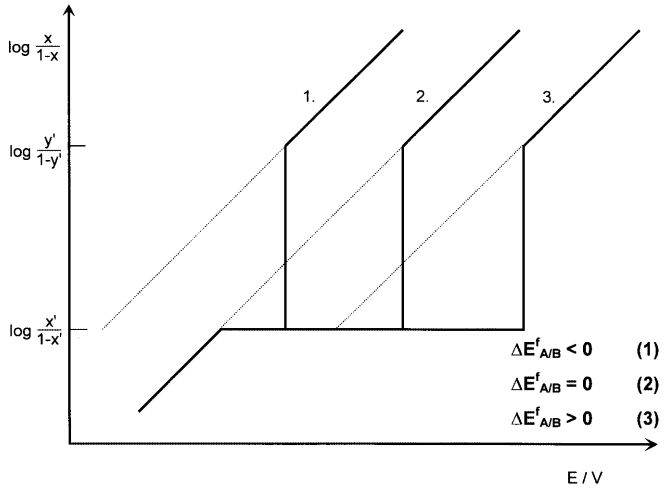

Fig. 2 A scheme of immiscibility gaps

$$\Delta G_{A/B} = \Delta G_{red/ox} + \Delta G_{lattice} \tag{22}$$

where $\Delta G_{red/ox}$ is the change in free energy due to the different redox composition (or, in other terms, due to the different activity of the intercalating guest C^+ in the host lattice) and $\Delta G_{lattice}$ is the difference in free energy due to the different structures of the lattice. In a Gedankenexperiment, $\Delta G_{lattice}$ is the free energy of transformation of phase α into β without changing the composition of α. $\Delta G_{lattice}$ may have very different values. If β is much more stable than α, this will shift the formal potential of the red/ox system in this phase so much in comparison to its value in phase α that within the miscibility gap the phase β will be formed at the expense of α until all α is converted to β (curve 1 in Fig. 2). The free energy of formation of β will shift the formal potential of red/ox in β to much more negative potentials in comparison to its value in α. This is very similar to the classical case of an electrode of the second kind, i.e. the formation of a very stable solid phase, usually a precipitate of low solubility, keeping the activity of a redox species at a low concentration. This is also what is usually discussed in relation to intercalation electrochemistry when phase segregation is discussed [2]. However, what happens when $\Delta G_{lattice}$ is very small compared to $\Delta G_{red/ox}$, i.e., when it is equivalent to some mV only? This question is interesting because many phase transformations of solids are known to be accompanied by changes in free energy of the order of some single or tens of kJ/mol, which is equivalent to some ten mV only. In such cases it is reasonable to set $\Delta G_{A/B} = \Delta G_{red/ox}$, which is just the same as to say that the formal potentials of the redox systems in α and β are the same (curve 2 in Fig. 2). This leads to the situation that, within the miscibility gap, there is no sufficient stabilization of β for a phase segregation. One can give another reasoning: within the miscibility gap the potential corresponds to the composition neither of α nor of β. Thus no net oxidation of α to form β can take place and, provided that supersaturation is principally excluded, the miscibility gap is simply an inert zone where no reaction can proceed. This behaviour has been quantitatively modelled in the preceding paper [1]. A third case is also possible, i.e., when the phase α is much more stable than β. It follows that the formal potential of red/ox in α is more negative than in β. This again leads to a separation of the potential ranges in which oxidation of red can occur. After completing the oxidation of $\{C_n red\}$ up to the composition of $\{ox_{x'}(C_n red)_{1-x'}\}$ there will occur an inert zone until the formation of $\{ox_{y'}(C_n red)_{1-y'}\}$ may take place. This inert zone is bigger than the miscibility gap (see curve 3 in Fig. 2) by the difference in formal potentials of red/ox in α and β. The voltammetric behaviour of such a system would be equal to that described in [1] provided one performs the calculation with a corrected value:

$$\Delta E'_{misc} = \Delta E_{misc} + \Delta E^{f}_{A/B} \tag{23}$$

with ΔE_{misc} being the miscibility gap according to Fig. 2 and $\Delta E^{f}_{A/B}$ being the difference in formal potentials of red/ox in α and β.

Immiscibility can hinder transfer of ions by diffusion from one phase to the other across the interface. If this interface advances parallel to the crystal surface, which is facing the solution, i.e., in the x direction (cf. Fig. 1), high concentration gradients and flux densities are needed. However, it may be assumed that the electrogenerated phase α ($c_{ox} < Z_{ox/Cred}$) is separated from the bulk phase β ($c_{ox} > 1 - Z_{Cred/ox}$) by a certain transition zone inside which the structure of the β phase is destroyed, but the structure of the α phase is not yet established [7]. Within this zone the concentration of oxidized species can be lower than it is in the β phase, but higher than it is in the α phase ($Z_{ox/Cred} < c_{ox} < 1 - Z_{Cred/ox}$; see Fig. 3). Hence, the advancement of the α phase from the solution facing the crystal surface into the particle body is preceded by the expansion of the transition zone. This process can occur only at the electrode potential at which the α phase is stable because it is assumed that the reconstruction of the crystal

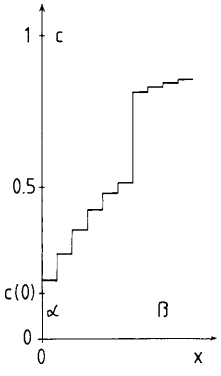

Fig. 3 Concentrations of the oxidized solid component {ox} in the vicinity of the crystal surface facing the solution. The surface concentration $c(0)$ and the α and β phases are marked. The electrode potential is −0.0448 V vs. E°_{f}. Miscibility limits: $Z_{Cred/ox} = Z_{ox/Cred} = 0.2$, $d = 0.4$, $\Delta E = 0.0002$ V and $n = 500$

structure is initiated by the appearance of the α phase on the particle surface, which is in contact with the solution. The propagation of electrons and counter ions through the particle body was simulated by a simple assumption of a thin layer (3–5 space increments wide) within which electrons and counter ions can freely diffuse without the restrictions imposed by the limited miscibility of the reduced and oxidized species. At the interface between the β phase and the transition zone, the concentration barrier is stable if the difference between the concentrations of the oxidized species is not bigger than a certain critical value [e.g. $c(j+1) - c(j) \leq 0.3$; see Fig. 3]. The transition zone advances when the barrier collapses. Its boundary to the α phase is diffuse. The results of the simulation are shown in Fig. 4. The cyclic voltammogram consists of four peaks. This response was calculated by assuming equal maxima miscibilities $Z_{\mathrm{Cred/ox}} = Z_{\mathrm{ox/Cred}} = 0.2$. This means that the mixed crystal is saturated with $\{C_n\mathrm{red}\}$ when 20% of $\{\mathrm{ox}\}$ is reduced. The first peak on the cathodic branch of the voltammogram corresponds to the first critical potential at which the surface of the crystal is saturated by the reduced component: $E_{\mathrm{C},1} = E_{\mathrm{f}}^{\circ} + (RT/nF)\ln[(1 - Z_{\mathrm{Cred/ox}})/Z_{\mathrm{Cred/ox}}]$. The composition of the crystal surface remains constant and independent of the electrode potential until the potential is equal to the second critical value $E_{\mathrm{C},2} = E_{\mathrm{f}}^{\circ} + (RT/nF)\ln[Z_{\mathrm{ox/Cred}}/(1 - Z_{\mathrm{ox/Cred}})]$ at which the composition is abruptly changed to 80% $\{C_n\mathrm{red}\}$ and 20% $\{\mathrm{ox}\}$. At $E_{\mathrm{C},2}$ the second peak appears. The remaining response is caused by the diffusion of ions into the product phase. It is characterized by current oscillations, which are caused by the fluctuation of concentrations in the transition zone. Figure 5 shows a detail of the response including the second peak. It consists of sharp spikes and oscillations with decreasing amplitudes. This vibration is a consequence of a development of the transition zone. This can be seen in Fig. 6. At −0.0360 V vs. E_{f}° (a), a relatively high concentration of the oxidized species near the crystal surface causes the spike appearing at −0.0362 V (see Fig. 5) and the decrease of the surface concentration (b). At −0.0364 V (c) the concentration barrier becomes unstable and collapses at −0.0366 V (d). This perturbation increases slightly the surface concentration at −0.0368 V (e), which causes the current spike at −0.0370 V (f). The second wave of oxidized species arrives at the surface at −0.0372 V and

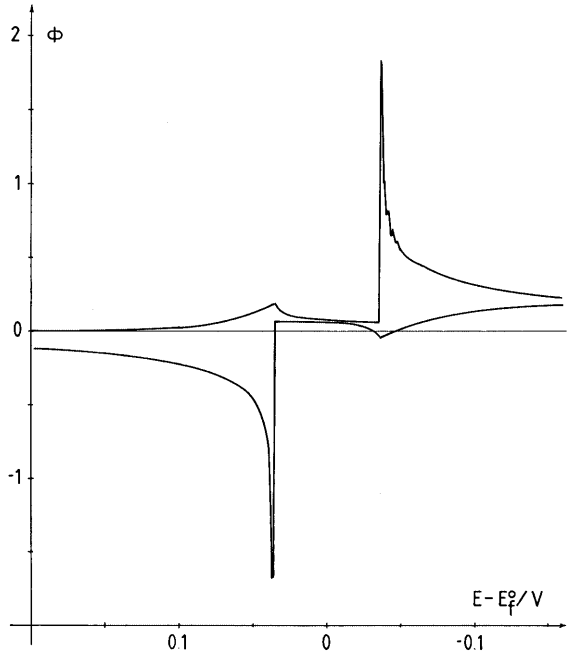

Fig. 4 Cyclic voltammogram of partly immiscible redox components. Reversible redox reaction. Miscibility limits: $Z_{\mathrm{Cred/ox}} = Z_{\mathrm{ox/Cred}} = 0.2$, $d = 0.4$, $\Delta E = 0.0002$ V and $n = 500$

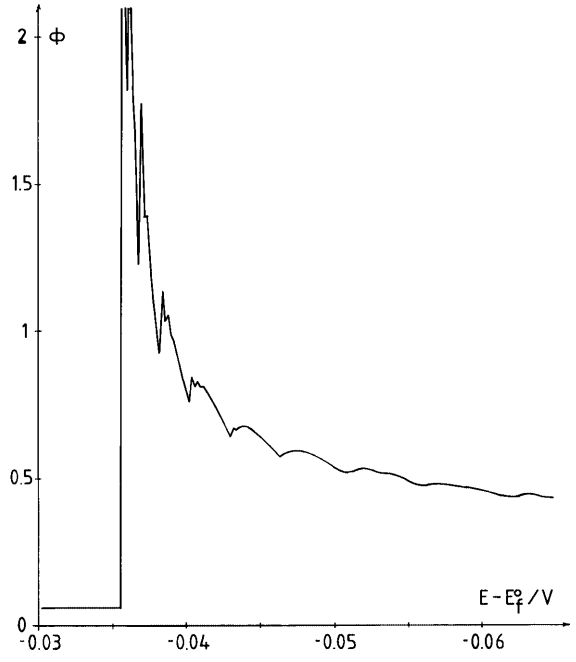

Fig. 5 A detail of the voltammogram shown in Fig. 4. All data as in Fig. 4

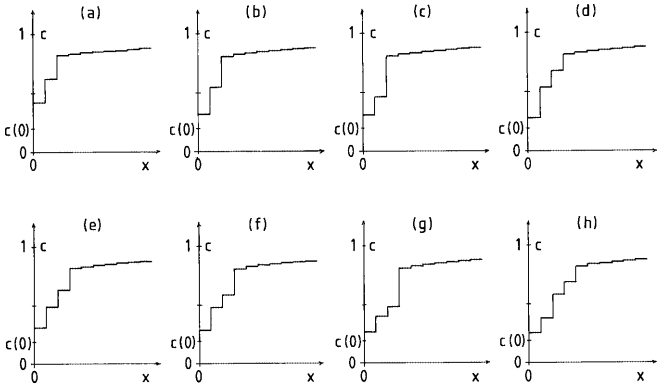

Fig. 6 Concentrations of the oxidized solid component $\{\mathrm{ox}\}$ as a function of electrode potential: $E - E_{\mathrm{f}}^{\circ}/\mathrm{V} = -0.0360$ (**a**), −0.0362 (**b**), −0.0364 (**c**), −0.0366 (**d**), −0.0368 (**e**), −0.0370 (**f**), −0.0376 (**g**) and −0.0378 (**h**). All other data as in Fig. 4

causes a small spike at −0.0374 V (Fig. 5). The collapse of the barrier, which occurs at −0.0378 V (Fig. 6, h) is a perturbation, which needs a longer time to reach the surface, and hence the corresponding spike appears at −0.0384 V (Fig. 5).

If the stability of the concentration barrier is smaller, the transition zone is wider and the propagation of electrons and counter ions is faster. Under the condition of a diffuse boundary between the transition zone and the β phase, the response is smooth, as can be seen in Fig. 7. In the reverse branch of the cyclic voltammogram the first peak appears at the potential $E_{C,2}$ which corresponds to the oxidation of $\{C_n red\}$ within the α phase. The second peak at $E_{C,1}$ marks the formation of the β phase on the crystal surface. The rest of the response is a consequence of the diffusion of electrons and counter ions from the particle body towards the crystal surface.

The difference between the potentials of the first and the second peaks depends on the maximum miscibility of the oxidized and reduced species. Figure 8 shows the cyclic voltammogram, which was simulated assuming rather high maxima miscibilities ($Z_{Cred/ox} = Z_{ox/Cred} = 0.4$) and a very wide transition zone with diffuse boundaries with both the α and β phases. This response can be compared with the opposite case in which no existence of any transition zone was assumed. Under these conditions, the voltammetric response is influenced by concentration barriers at the interface between the α and β phases. A theoretical cyclic voltammogram influenced by a limited mutual solubility of the solid redox components is shown in Fig. 9. It was calculated for the same maxima miscibilities as in Fig. 8, but no transition

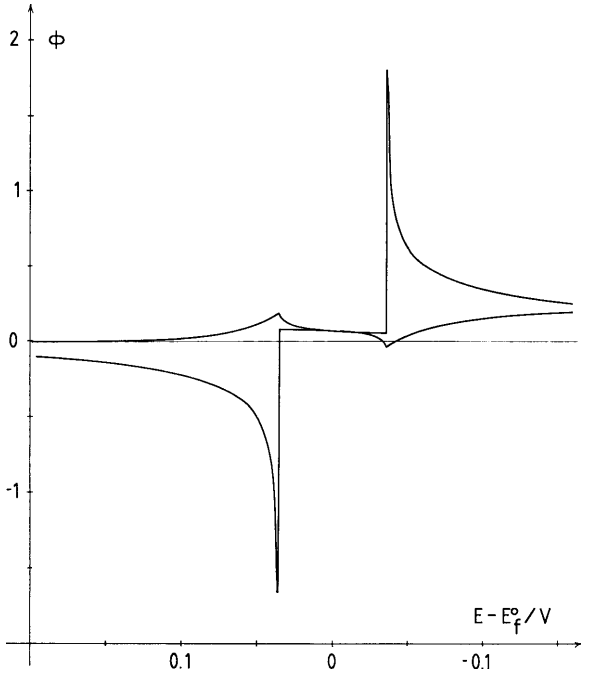

Fig. 7 Cyclic voltammogram of partly immiscible redox components. Reversible redox reaction. Miscibility limits: $Z_{Cred/ox} = Z_{ox/Cred} = 0.2$. All other data as in Fig. 4

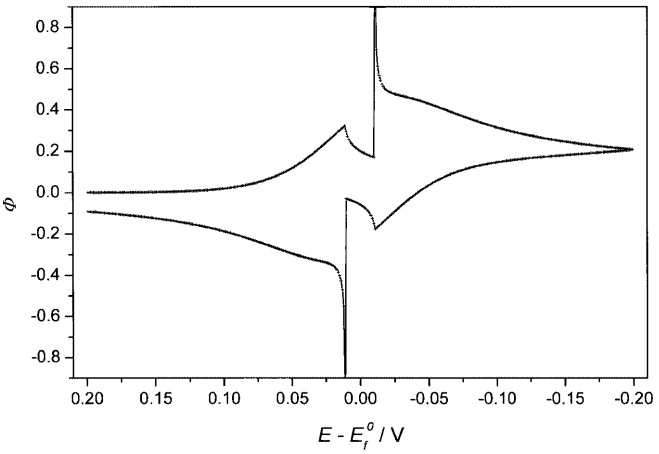

Fig. 8 Cyclic voltammogram of partly immiscible solid redox components. Reversible redox reaction. Miscibility limits: $Z_{Cred/ox} = Z_{ox/Cred} = 0.4$, $d = 0.4$, $\Delta E = 0.0002$ V and $n = 100$

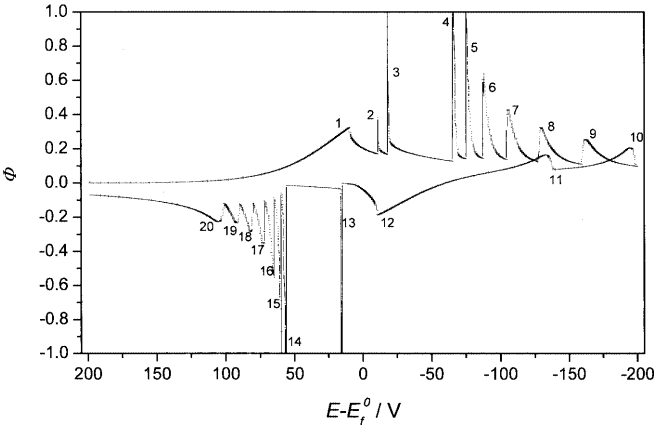

Fig. 9 Cyclic voltammogram of partly immiscible solid redox compounds. Reversible redox reaction. Miscibility limits: $Z_{Cred/ox} = Z_{ox/Cred} = 0.4$, $d = 0.4$, $\Delta E = 0.0002$ V and $n = 100$. No transition zone was assumed

zone was assumed. The first two peaks on the cathodic branch of the voltammogram appear at the critical potentials $E_{C,1}$ and $E_{C,2}$, respectively. However, the potential $E_{C,2}$ is not sufficient to initiate the massive ingress of cations, which is necessary for the collapse of the first concentration barrier [Eqs. (16) and (17)]. This collapse is marked by the third peak. The corresponding concentration profiles are shown in Fig. 10A. The peaks 4–9 mark the collapses of the second to the seventh barriers. The changes of concentrations of the oxidized solid component {ox} near the crystal surface facing the solution during the collapse of the concentration barrier are given in Table 1 and Fig. 11. The more distant the barrier, the more delayed and longer is the current response. So, the peaks corresponding to distant barriers are wider than the peaks caused by the collapse near to the surface barriers. The collapse of the barrier is an advancement of the phase boundary. If the density of flux at a certain moment is constant over the whole

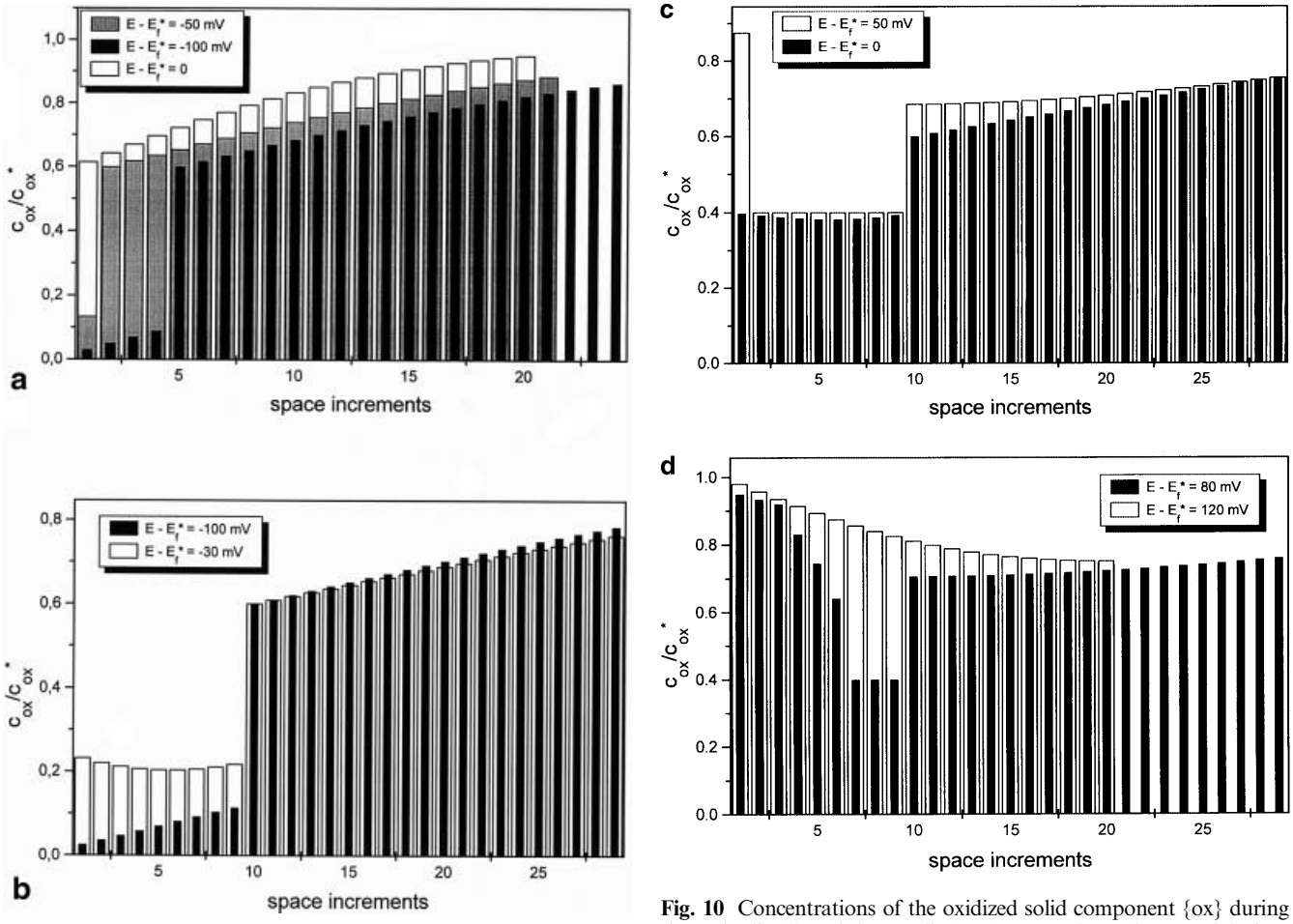

Fig. 10 Concentrations of the oxidized solid component {ox} during the cathodic (**a**) and the anodic (**b–d**) scans. Electrode potentials: in **a** $E/\mathrm{V} = 0, -0.05, -0.1$; in **b** $-0.1, -0.03$; in **c** 0, 0.05; in **d** 0.08, 0.12. All other data as in Fig. 9

boundary, the collapse occurs when the difference in concentration at the barrier is so high as to induce the flux which satisfies the conditions of Eqs. (16) and (17), or Eqs. (20) and (21) respectively.

At the beginning of the anodic branch of the cyclic voltammogram the barrier collapse continues (peaks 10 and 11). The corresponding concentration profiles are shown in Fig. 10B. At the second critical potential the crystal surface is saturated by the oxidized component {ox} and peak 12 appears. In the potential range between $E_{C,2}$ and $E_{C,1}$ (diagram 1 in Fig. 10C), this saturation is extended from the surface to the concentration barrier. So, when the composition of the mixed crystal on the particle surface is abruptly changed at $E_{C,1}$, the current response is negligible because at this potential the concentration difference is not high enough to induce

Table 1 Collapse of the barrier

$(E - E_f^*)$(V)						
−0.0736	−0.0738	−0.0740	−0.0742	−0.0744	−0.0746	
$c(x)/\rho$						x
0.0636	0.0631	0.0627	0.1423	0.1100	0.1220	1
0.0825	0.0821	0.2817	0.2414	0.2562	0.2301	2
0.6000	0.6000	0.3999	0.3774	0.3371	0.3159	3
0.6178	0.6178	0.6177	0.6000	0.6000	0.6000	4
0.6355	0.6354	0.6353	0.6352	0.6281	0.6266	5
0.6530	0.6529	0.6527	0.6526	0.6525	0.6496	6
0.6702	0.6700	0.6698	0.6697	0.6696	0.6694	7
0.6870	0.6868	0.6866	0.6864	0.6863	0.6861	8
0.7033	0.7031	0.7029	0.7027	0.7026	0.7024	9
0.7192	0.7190	0.7188	0.7186	0.7184	0.7182	10
Φ						
0.1438	0.1433	0.1429	1.2898	0.8316	1.0101	

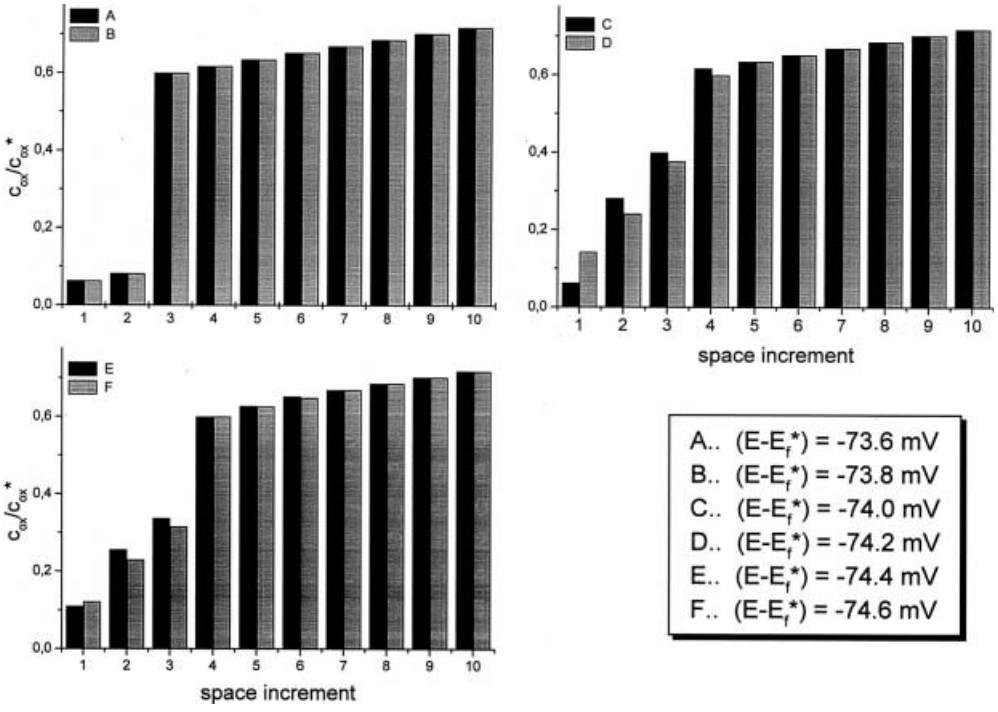

Fig. 11 Concentrations of the oxidized solid component {ox} during the collapse of the barrier (see text)

the collapse of the first anodic barrier. The collapse occurs at 0.016 V (peak 13 in Fig. 9 and profile 2 in Fig. 10C). The collapses of other barriers are marked by a series of peaks 14–20. The spikes in the voltammogram are not artefacts of the simulation but they originate from overcoming the concentration barriers. The typical concentration profiles are shown in Fig. 10D.

The concentration barrier can collapse if Eq. (17) is satisfied. This condition can be written in the form

$$c(j) = [Z_{\mathrm{ox/Cred}} - (1-d)(1-Z_{\mathrm{Cred/ox}})]/d \qquad (24)$$

Equation (24) satisfies also the inequality of Eq. (16). Equation (24) has a physical meaning only if $c(j) > 0$ and hence:

$$Z_{\mathrm{ox/Cred}} > (1-d)(1-Z_{\mathrm{Cred/ox}}) \qquad (25)$$

where $0 < d < 0.5$. If $Z_{\mathrm{Cred/ox}} = Z_{\mathrm{ox/Cred}}$, then:

$$Z_{\mathrm{ox/Cred}} > (1-d)/(2-d) \qquad (26)$$

So, $Z_{\mathrm{ox/Cred}} > 0.33$ and $b < 0.33$. This analysis indicates that in the case of low miscibility of the redox components ($Z_{\mathrm{Cred/ox}} \leq 0.3$ and $Z_{\mathrm{Cred/ox}} = Z_{\mathrm{ox/Cred}}$) the solid compound exhibits no ionic conductivity because the concentration gradients developing within the solid particle are not high enough to initiate the fluxes, which satisfy Eqs. (16) and (17), or (20) and (21) respectively.

Conclusions

This theoretical study demonstrates the thermodynamic conditions that must be fulfilled for the occurrence of a miscibility gap of solid phases. When the free energy change accompanying the phase transformation is negligibly small, the formal potentials of the redox system will be equal in both phases. Provided that the compounds have sufficient conductivity, this leads to the impossibility of coexistence of the two phases α and β on the surface of the electrode. The miscibility gap between the two phases on the potential axis is therefore an inert zone. Only after surpassing the inert zone can the electrochemical reaction advance into the solid with the development of the transition zone between the α and β phases. When one fully excludes the transition zone, the electrochemical reaction can only advance through the solid for a miscibility gap smaller than 0.33. Even then, the reaction has to overcome concentration barriers, which show up in the form of strange spikes in the voltammogram. However, a development of sharp interfaces within redox active solid compounds is less probable than the appearance of diffuse interfaces between the α and β phases [7]. This may be a reason why there is no experimental evidence for the coupled transport of ions and electrons, which is hindered by concentration barriers. To our best knowledge, no system has been reported which exhibits such behaviour.

Acknowledgements This research was funded by *Deutsche Forschungsgemeinschaft*, which is gratefully acknowledged. Further support by the respective Ministries in the framework of a bilateral German-Croatian Scientific Research Program and by *Fonds der Chemischen Industrie* is acknowledged.

References

1. Scholz F, Lovrić M, Stojek Z (1997) J Solid State Electrochem 1: 134

2. McKinnon WR (1995) Insertion electrodes I: atomic and electronic structure of the hosts and their insertion compounds. In: Bruce PG (ed) Solid state electrochemistry. Cambridge University Press, Cambridge, pp 163–198
3. Scholz F, Dostal A (1995) Angew Chem 107: 2876
4. Jaworsky A, Stojek Z, Scholz F (1993) J Electroanal Chem 354: 1
5. Lovrić M, Scholz F (1999) J Solid State Electrochem 3: 172
6. Britz D (1988) Digital simulation in electrochemistry. Springer, Berlin Heidelberg New York
7. Sutton AP, Balluffi RW (1995) Interfaces in crystalline materials. Oxford, University Press, Oxford, pp 241–247